JOURNAL OF PROPULSION AND POWER
Vol. 31, No. 5, September–October 2015

Experimental Validation of Numerical Blade Flutter Prediction

Vasily V. Vedeneev* and Mikhail Kolotnikov†
Lomonosov Moscow State University, 119991, Moscow, Russia
and
Pavel Makarov‡
Gas Turbine Engineering Research and Production Center, Salut, 105118, Moscow, Russia

DOI: 10.2514/1.B35419

Blade flutter of modern gas-turbine engines is one of the main issues that engine designers have to face. The most used numerical method that is employed for flutter prediction is the energy method. Although a lot of papers are devoted to the analysis of different blade wheels, this method was rarely validated by experiments. Typical mesh size, time step, and various modeling approaches that guarantee reliable flutter prediction are not commonly known, whereas some examples show that predictions obtained through nonvalidated codes can be inaccurate. In this paper, we describe our implementation of the energy method. Analysis of convergence and sensitivity to various modeling abstractions are carefully investigated. Numerical results are verified by compressor and full engine flutter test data. It is shown that the prediction of flutter onset is rather reliable so that the modeling approaches presented in this paper can be used by other researchers for the flutter analysis of industrial compressor blades.

Downloaded by UNIVERSITY OF CAMBRIDGE on August 21, 2015 | http://arc.aiaa.org | DOI: 10.2514/1.B35419

Nomenclature

f	=	natural frequency
m	=	number of nodal diameters
N	=	number of blades
n	=	rotor speed
W	=	work done by the unsteady pressure over one cycle of blade oscillation
α	=	inlet angle of attack
φ	=	2π m/N, interblade phase shift
ω	=	$2\pi f$, circular frequency

I. Introduction

AIRCRAFT gas-turbine engine designers were faced with compressor blade flutter in the middle of the 1950s while developing the second generation of jet engines. At the present day, a huge theoretical and practical experience has been accumulated. Typically, regions of the various flutter types are plotted on the compressor operating map. They were developed by different researchers and are very similar [1–5]. The scheme in Fig. 1 proposed in [2] can be considered as a typical example. This map clearly shows that possible flutter regions are mainly located near the surge line or significantly lower than the compressor operating line. When operating in these regions, the airflow in the blade passages is unsteady, including unsteady recirculation zones and possibly shocks. The only exceptions are the regions bounded by lines 3, 4, and 6. They lead to the blade flutter near the operating line for unstalled flow. Recently, it was demonstrated [6] that the region bounded by line 2 can also be located near the operating line, and the flow can be continuous.

The problem of numerical flutter prediction for the compressor or fan blade wheels is associated with the coupled aeroelastic problem, which first needs a solution for a steady-state flow in blade passages. Modern computational codes, such as Ansys CFX, Star-CCM, Fluent, FlowVision, etc., provide reliable airflow parameters in blade passages near the operating line, where the flow is unstalled. For surge line (region 1) and for stalled flow (regions 2, 5, and 7), it is very difficult (and usually impossible) to determine reliable airflow parameters numerically, which is why the numerical prediction of blade flutter boundaries for these regions usually cannot give any valid results. However, for the design phase of modern gas-turbine engine compressors and fans, the most important is to suppress flutter around the operating line with required safety margins because this provides the ability for test validation of the main characteristics of the new compressors. The dynamic stress state of compressor or fan blades operating near the surge line and in regions of stalled flow is typically determined experimentally during the refinement of the engine.

Basically, there are four methods for flutter prediction [3,4]. The first (direct) method is based on the direct time-domain numerical simulation of a coupled blade-flow system. This method not only provides flutter regimes but also gives limit cycle amplitude if flutter occurs [7]. However, numerical difficulties of this approach and the necessity of a great amount of computational resources and time are the main limitations of the wide applications of this method. Also, it is not easy to understand the physical nature of vibration amplification and adequately redesign the blade if flutter occurs.

The second (frequency or modal) method is based on the calculation of the eigenfrequencies of a coupled fluid–structure system. Generally, the eigenfrequencies of such system are complex because the system is not conservative. The positive imaginary part of the eigenfrequency is a criterion for flutter. This method is rather common and can be applied to the flutter prediction of any aeroelastic structure. However, there are mathematical issues with finding the eigenvalues of complex nonsymmetric matrices [8]; also, computational resources comparable with the first method are necessary.

The third (energy) method is based on the calculation of the work done by the gas forces on the displacements of the elastic blade oscillating in a natural mode over one cycle of oscillation. This method provides acceptable results if the natural mode shapes in vacuum and in flow are similar, which is almost always true, except for hollow blades. If the work is positive and greater than the work of damping forces, then flutter occurs. The advantage of this approach is that the analysis is relatively quick; only modal analysis should be conducted for elastic blades, whereas the calculation of the work is a purely aerodynamic problem. The problem is uncoupled, and time savings are significant.

The fourth method of flutter prediction is the most used by gas-turbine engineers and is based on the results of the analysis and synthesis of practical experience of flutter occurrence in the compressor and fan blades of real gas-turbine engines after their refinement and in service. To formulate a criterion of flutter initiation, both deterministic and probabilistic methods are used. Such criteria are mainly one- or two-parametrical, though there are criteria with many more parameters [9,10]. For each type of flutter, the system of

Received 10 April 2014; revision received 19 February 2015; accepted for publication 10 March 2015; published online 20 May 2015. Copyright © 2015 by Vasily Vedeneev, Mikhail Kolotnikov, and Pavel Makarov. Published by the American Institute of Aeronautics and Astronautics, Inc., with permission. Copies of this paper may be made for personal or internal use, on condition that the copier pay the $10.00 per-copy fee to the Copyright Clearance Center, Inc., 222 Rosewood Drive, Danvers, MA 01923; include the code 1533-3876/15 and $10.00 in correspondence with the CCC.

*Associate Professor, Faculty of Mechanics and Mathematics.
†Professor, Institute of Mechanics.
‡Head, Stress Department.

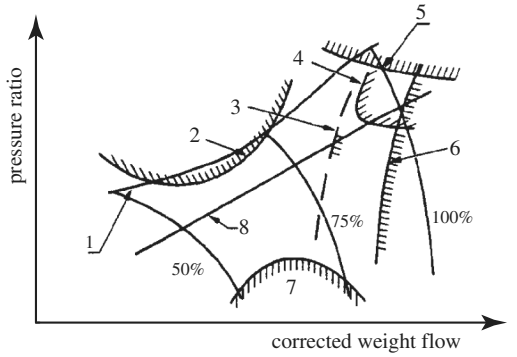

Fig. 1 Compressor map [2]: 1) surge line, 2) subsonic stalled flutter, 3) bending–torsional flutter, 4) supersonic unstalled flutter induced by shocks, 5) supersonic stalled flutter, 6) supersonic unstalled flutter, 7) choking flutter, and 8) operating line.

Downloaded by UNIVERSITY OF CAMBRIDGE on August 21, 2015 | http://arc.aiaa.org | DOI: 10.2514/1.B35419

parameters is supplemented with limit values, established from the study and generalization of flutter onset conditions in compressors-prototypes. These limits bound a possible flutter zone. One of the simplest criteria is the reduced frequency (Strouhal number) $Sh = \omega b/V$, where b is the blade chord of peripheral cross section, ω is the circular blade frequency, and V is the flow speed. Shrinivasan reported [4] that, for guaranteed flutter suppression in bending mode, Sh must be greater than 0.8; for torsional mode, it must be greater than 1.4. The wide application of this method by gas-turbine engine engineers is reasonable because it provides the ability to use huge experience that has been accumulated from engine prototypes. On the other hand, such criteria should be used very carefully by engineers from other companies because they can give an unrealistic prediction for different compressor designs and operating parameters.

Because the fourth method is not applicable to essentially new blade designs, a great effort has been made over decades to develop numerical codes for predicting flutter using the first three methods. We will give a very brief overview of such codes; the most comprehensive reviews on computational aeroelasticity in turbomachinery can be found in [3,11].

Many of the numerical codes are two-dimensional, including those based on the energy and modal methods [12–17]. As a rule, in such studies, a two-dimensional (2-D) cross section at 80–100% of the blade span is modeled, which implies that this cross section governs the overall stability of the blade. This approach is reasonable for theoretical investigations of general effects, such as the effect of the mode shape, interphase blade angle, cascade mistuning, etc. However, for real compressor or turbine blades, which are essentially three-dimensional (3-D), there are usually no arguments to choose a particular cross section. Moreover, in Sec. IV.E, we will give an example of a blade whose overall stability prediction does not coincide with the prediction obtained through the 2-D cross section taken at 90% of the blade span. At the present day, the 2-D approach is verified by tests of cylindrical blades (i.e., blades whose cross section is constant along the span) [18–24]. A study [25] is devoted to the comparison of energy and modal methods based on a quasi-3-D approach. It is shown that, for sufficiently stiff metal blades, the energy method gives results very close to those obtained by the modal method, but for a more flexible composite blades, the inaccuracy of the energy method, caused by the difference of the mode shapes in the flow and in vacuum, is more pronounced.

Starting from a series of papers [26–29] as well as [30,31], several 3-D aeroelastic codes have been developed by different researchers during the last decade [32–37]. Most of them are based on the energy method, though there are some employing time-domain and eigenfrequency calculations. However, many of the 3-D codes are not carefully validated by experiments, and some are not verified at all. The most impressive evidence of uncertainty of unvalidated codes is the comparison of aerodynamic damping calculations for the same test object conducted by five different partners of the FUTURE project [38]: the spread of predictions is of 100% of the damping magnitude; two of the five calculations predict flutter, whereas three predict stability. As the authors of [38] note, "On the background that all these partners are known experts in aircraft engine components, these results underline the uncertainty presently associated with flutter predictions".

In the open literature, only a few papers are devoted to the comparison of numerical and test data for 3-D blades [39–42]. All the authors of those papers compare calculated and measured aerodynamic damping (i.e., in fact, they validate aeroelastic codes based on the energy method). Although a good correlation is obtained, the aforementioned note [38] should not be ignored: a significant difference between the predictions shows that validations of numerical codes by experiments must be conducted, and reliable parameters of the numerical schemes used should be elaborated during such validations.

In this paper, we implement the energy method in 3-D formulation for blade flutter analysis, which uses unsteady aerodynamics from the industry-recognized code Ansys CFX. We investigate the influence of modeling different features: number of blades simulated, modeling of the blade shroud, and effects of manufacturing tolerances, expressed in the distortion of the blade mode shapes, tension in the blade shroud, and the inlet angle of attack. Results are validated by test results obtained for two blade wheels. Each wheel is tested and numerically analyzed at two regimes, one of which is stable and the other is the flutter regime. Numerical parameters used in calculations and the influence of various modeling features validated in this paper can be used by other investigators for reliable predictions of the flutter onset.

The structure of the paper is as follows. First, in Sec. II, we describe in detail the energy method and formulate a step-by-step algorithm. Section III is devoted to a convergence study. In Sec. IV, we numerically analyze two blade wheels. Finally, in Sec. V, we present results of an experimental study of the wheels analyzed, which validate the method developed.

II. Method of Flutter Prediction

We assume that the influence of the flow on natural blade modes and frequencies is negligible. This assumption is valid for the case of sufficiently stiff blades, when flow disturbances excited by small blade vibration have no significant action on blade eigenmodes. Therefore, the airflow can result only in small additional damping (for stability case) or additional energy inflow (for flutter case) without change of natural modes and frequencies. The energy equation for a blade in a coordinate system rotating with the wheel is

$$\frac{\mathrm{d}E(t)}{\mathrm{d}t} = A(t) \tag{1}$$

where $E(t)$ is the total energy, and $A(t)$ is the power of internal and external forces. Neglecting structural damping and viscous forces of the flow, we assume that the only force is the air pressure distributed along the blade surface. Then the change of the total energy over the cycle of oscillation is

$$\Delta E = W = \int_{t_0}^{t_0+T} \int_{S} p(x,y,z,t)\boldsymbol{n}(x,y,z,t)\boldsymbol{v}(x,y,z,t)\,\mathrm{d}s\,\mathrm{d}t \tag{2}$$

where $T = 1/f$ is the blade oscillation period (f is the natural frequency), S is the blade surface, p is the flow pressure, $\boldsymbol{n}$ is the blade surface normal, and $\boldsymbol{v}$ is the velocity of the blade points.

Since the flow influence on the blade oscillations is small, the work W done over actual (growing or damped) oscillation is also small. The work over harmonic (i.e., constant amplitude) oscillation is different from the actual work by a second-order infinitesimal term, which is neglected. Harmonic oscillation shape is assumed to be obtained from the modal analysis of the blade in vacuum using standard engineering software.

Thus, we calculate the work done by pressure over specified oscillations of the blade during one oscillation period. The following inequality is a criterion of flutter:

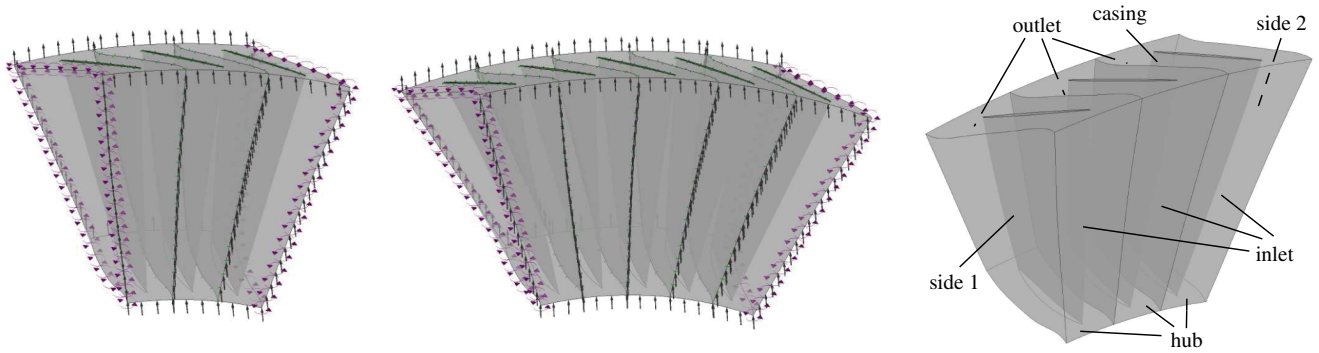

Fig. 2 Models of consecutive blade passages: a) three, b) five; and c) boundary conditions.

Downloaded by UNIVERSITY OF CAMBRIDGE on August 21, 2015 | http://arc.aiaa.org | DOI: 10.2514/1.B35419

$$W > 0 \tag{3}$$

The finite-volume model of the flow consists of three or five consecutive blade passages of one stage (Figs. 2a and 2b). For unsteady fluid flow analysis, initial and boundary conditions are extracted from steady-state flow calculated for the full compressor (where all stages are modeled), verified by full-scale compressor tests. Namely, we specify the distribution of the total pressure, total temperature, velocity, and turbulence parameters at the inlet (Fig. 2c) and distribution of static pressure at the outlet. A no-slip condition is assigned at solid body surfaces: hub, blades, and casing; for the latter surface, the no-slip condition is applied in the counterrotating coordinate system. The condition of rotational periodicity connects flow parameters at sides 1 and 2 (Fig. 2c). Note that latter boundary condition (the only available in the aerodynamic code used) distorts the traveling wave in the flow, so that it is necessary to model several consecutive blade passages and calculate the work done over the middle blade, which is the most remote from sides 1 and 2. For codes where the phase lag between sides 1 and 2 can be taken into account, one passage is enough for the modeling the traveling wave.

Mesh displacement in the form of the wheel natural mode with a specified number of nodal diameters is applied to each blade surface: $\boldsymbol{u}(x, y, z, t) = A \sin \omega t \times L_n(x, z)$, where A and $\omega = 2\pi f$ are the blade oscillation amplitude and circular frequency, and $L_n(x, z)$ is a function representing the mode shape. We use the 10th-order Lagrange interpolation polynomial for interpolating finite-element mode shape results and transferring them to the computational-fluid-dynamics code.

For modeling a forward (or backward) traveling wave, which is typical for compressor blade flutter [43], phase lag sin $(\omega t - \varphi)$ and lead sin $(\omega t + \varphi)$ with respect to the middle blade are specified for neighboring blades, where the phase shift $\varphi = 2\pi$ m/N corresponds to the number of nodal diameters m. In the case of the five-blade model, the phase shift for the side blades is $\pm 2\varphi$.

Let us prove that with these assumptions the work done by a steady component of pressure over one cycle of harmonic oscillation is zero. Indeed, the work associated with the steady pressure can be nonzero only if there is a phase shift between different blade points (i.e., eigenmodes are complex) [44]. However, we assume that each blade oscillates in the form of a standing wave, such that there is no phase shift between points of the same blade (though the phase shift between different blades is nonzero); hence, the eigenmodes are real. In this case, the work done by the steady pressure is zero. Therefore, we will assume that the pressure p in Eq. (2) is the unsteady portion of the pressure caused by blade oscillation.

In accordance with the procedure described, flutter analysis consists of four stages: 1) modal analysis of elastic blades, interpolation of mode shapes by Lagrange polynomials; 2) steady-state flow analysis in compressor; 3) unsteady flow analysis of a certain compressor stage with blades oscillating (i.e., fluid mesh moving) in a specified mode obtained in step 1; and 4) the calculation of work [Eq. (2)] done by pressure for the middle blade and check of criterion (3).

Steps 3 and 4 are executed for each natural mode potentially sensitive to flutter. Work is calculated for the last of several simulated cycles of oscillations, such that the flow response to the blade oscillations is pure harmonic. Calculations show that three periods are typically enough to have a harmonic response (see Sec. III).

A structural modal analysis is performed using the Ansys Mechanical finite-element software. For fluid flow analysis, we use Ansys CFX, version 12.1. Reynolds-averaged Navier–Stokes (RANS) equations with $k - \varepsilon$ turbulence model are solved. For polynomial interpolation and calculation of work done by unsteady pressure, special in-house codes have been developed.

Flutter onset predictions and test data presented in this paper are obtained for two wheel models representing two stages of the same compressor (Table 1, index "0.5" means the middle of the blade span). Each wheel is analyzed in two configurations:

1) Wheel 1 with shrouded and with cantilever blades (Fig. 3a). The cantilever blade wheel is a special test wheel with blade shrouds cut to be out of contact with other blade shrouds. This wheel represents wear of material in contact pairs of the shroud. A fixed rotation speed specific for the throttle regime (compressor operating near region 3 in Fig. 1) is studied. Airflow parameters correspond to zero altitude and zero Mach number at the engine inlet. The flow at the stage inlet is transonic, with average Mach number $M \approx 0.9$ and 0.95 at 50 and 90% of the blade span, respectively. The flow at the blade passage has a certain supersonic region (Fig. 4).

2) Wheel 2 with shrouded blades (Fig. 3b). Rotor speeds $n =$ 159.5 and 170 Hz are analyzed. In the first case, the average Mach number at the stage inlet is subsonic, $M \approx 0.7$ and 0.9 at 50 and 90% of the blade span, respectively; in the second case, the flow is supersonic: $M \approx 1.2$ and 1.4. The flow in the interblade passage is fully subsonic in the first case and has a significant supersonic portion in the second case (Fig. 5). Because of the closeness of the physical rotation speeds, we assume that the blade natural modes and frequencies are the same and consider only the difference in the aerodynamics.

During the investigation of wheel 1, we studied numerical convergence and implementation features (number of blades in the model, oscillation amplitude, etc); results are compared with test data. During the analysis of wheel 2, we studied structural effects:

Table 1 Parameters of the wheels and regimes considered

Parameter	Wheel 1	Wheel 2
Number of blades (N)	45	37
Rotor speed n, Hz	136.0	159.5/170.0
Inner to outer diameter ratio d/D	0.570	0.435
Relative blade spacing $t_{0.5}/b_{0.5}$	0.800	0.766
Blade aspect ratio $h/b_{0.5}$	3.120	3.554
Midspan shroud location h_s/h	$0.710/(n/a)$	0.772

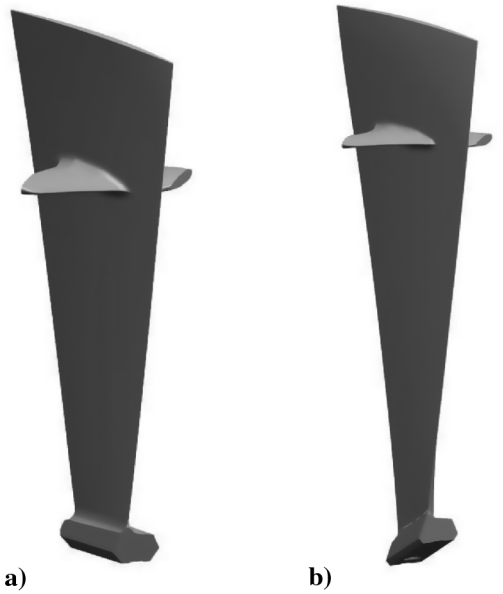

a) b)

Fig. 3 Blades of a) wheel 1, and b) wheel 2.

assembling force between contact surfaces of midspan shroud, deviation of the blade mode shape due to manufacturing tolerances, and inlet flow incidence angle.

To make sure that the steady aerodynamics, which is the basis for flutter analysis, is correctly obtained, let us consider the operating map of the compressor (Fig. 6), where the results of the numerical analysis and experimental points are shown. It is seen that the agreement between steady flow calculations and experiments is rather good. Thus, we consider the steady flow as correctly representing real airflow and can use it for unsteady flow analysis due to blade oscillations.

III. Analysis of Convergence and Numerical Effects

The three-blade model of wheel 1 was used for the analysis of convergence and the effect of numerical parameters. We calculated the work done by unsteady pressure over a cycle of oscillations in the first mode for $m = 0$ (all blades oscillate with the same phase).

The following parameters were selected as "basic" for the analysis. Single precision was used (all variables are of float type). Time step was $\Delta t = T/100$. Three periods were analyzed; work was calculated for the last period (i.e., for time steps 200 . . . 300). The rms convergence residual for RANS equations was set to be $5 \cdot 10^{-5}$ for each time step (maximum residual turns out to be $\sim 10^{-3}$). The number of internal iterations at each time step was higher than 10 and less than 100. The mesh consisted of approximately 200,000 control volumes per one blade passage (Fig. 7). Work calculated for the first natural mode is denoted by "1" in Fig. 8. For the investigation of

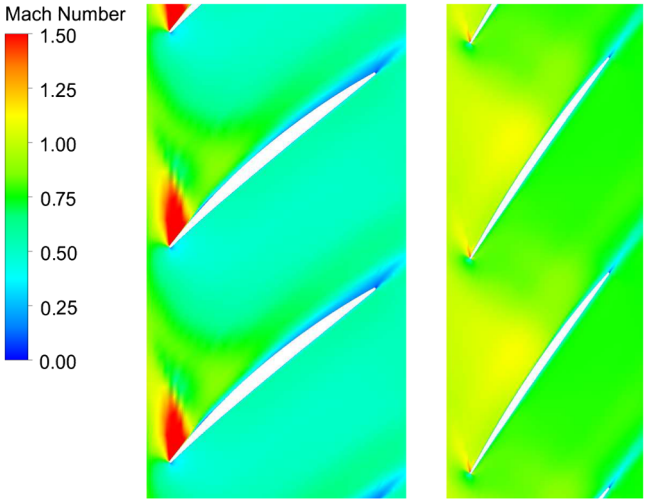

a) b)

Fig. 4 Mach-number distribution at wheel 1. Distributions at a) 50%, and b) 90% of the blade span are shown.

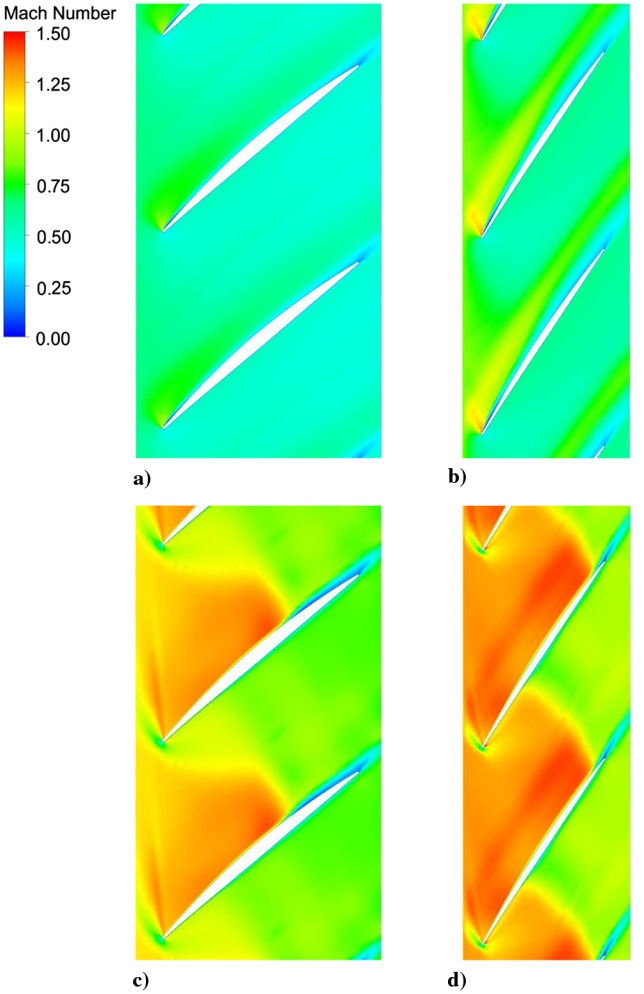

Fig. 5 Mach-number distribution at wheel 2 at regimes a–b) $n = 159.5$, and c–d) $n = 170$ Hz. Distributions at 50% (a,c) and 90% (b,d) of the blade span are shown.

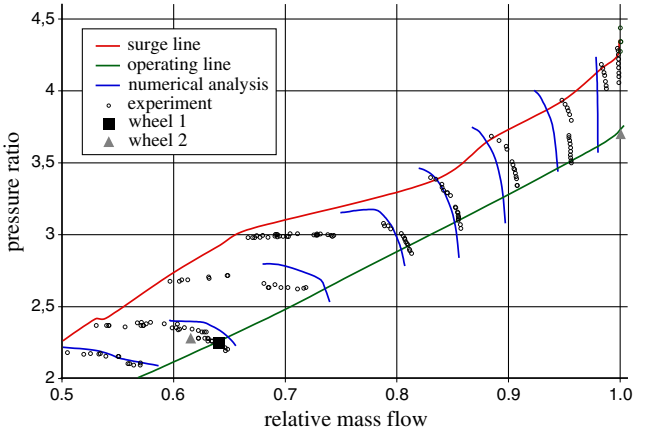

Fig. 6 Operating map of the compressor. Flow regimes corresponding to the analysis of wheels 1 and 2 are shown by black squares and gray triangles, respectively.

Downloaded by UNIVERSITY OF CAMBRIDGE on August 21, 2015 | http://arc.aiaa.org | DOI: 10.2514/1.B35419

Downloaded by UNIVERSITY OF CAMBRIDGE on August 21, 2015 | http://arc.aiaa.org | DOI: 10.2514/1.B35419

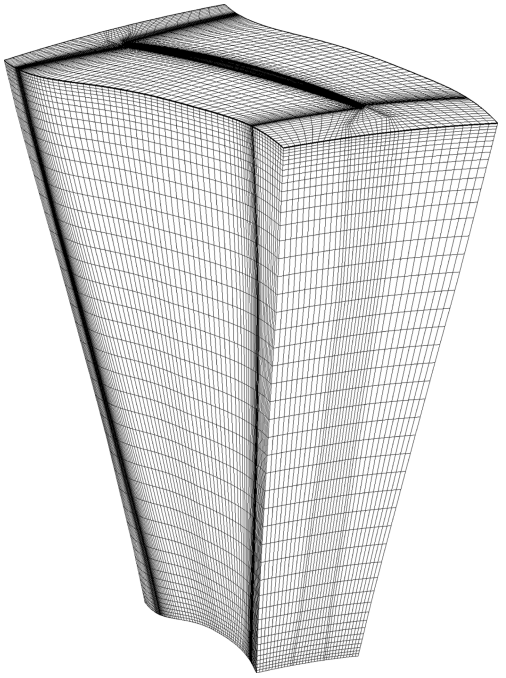

Fig. 7 Basic mesh (~200,000 control volumes per passage).

convergence, we calculated the same work with one of the parameters taken with higher precision. At each run, overall convergence criteria, such as integral conservation laws, were checked.

1) Precision of unsteady aerodynamic problem solution; calculations were conducted with double precision (all variables were of double type). Result is denoted by "2" in Fig. 8.

2) Convergence in time step; calculation with four-times-reduced time step, $\Delta t = T/400$, was conducted. Total simulation time (three periods) consisted of 1200 time steps. Result is denoted by "3" in Fig. 8.

3) Convergence in residuals; this case was checked together with the time step reduction. Result shown in Fig. 8, point "4", was obtained at a two-times-smaller time step (600 iterations for the full run time) and maximal residual of 10^{-4} (rms residual of $\sim 10^{-6}$).

4) Number of oscillation periods; to check the sufficiency of three periods for harmonicity of the flow at the last period, additional analysis was conducted with three more periods simulated. Work was calculated at the sixth period; result is denoted by "5" in Fig. 8.

5) Convergence in mesh; calculations were conducted using refined meshes of 430,000 and 800,000 control volumes per each blade passage. Results are shown in Fig. 8 as "6" and "7".

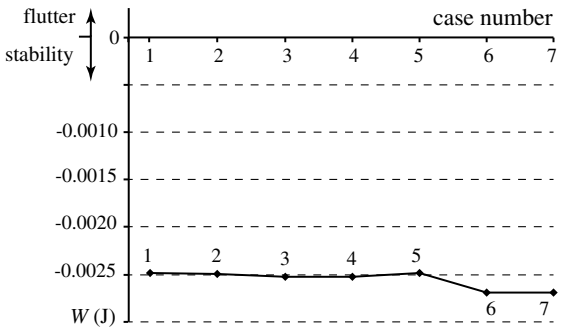

Fig. 8 Influence of numerical effects on the work done by unsteady aerodynamic pressure.

It is seen in Fig. 8 that the work done by pressure during the last oscillation period is changed insignificantly in all cases, except for a slight change due to mesh refinement; it proves the sufficiency of the basic parameters. To investigate mesh influence in more detail, we analyzed the whole range of nodal diameters for the first two natural modes. Results shown in Fig. 9, curves 1 . . . 3, represent mesh size of 200, 430, 800 thousands of volumes per blade passage. They prove that the convergence in mesh is achieved at a mesh size of 200,000 control volumes per passage.

The effect of the number of blades in the model (five-blade vs three-blade) was studied (Fig. 9, curve 4, mesh size is 200,000 volumes per passage) and appeared to be insignificant for the work. This means that only blades neighboring to the middle blade affect flutter. Thus, using a three-blade model is enough for a reliable flutter prediction. This result was also obtained in the investigation of aerodynamic influence coefficients in plate cascades [45].

Thus, convergence is verified, so that in studies described later, we use the basic parameters. The models consist of three blades; work-per-cycle is calculated for forward ($m > 0$) or backward ($m < 0$) traveling waves for the full range of nodal diameters.

IV. Results of Numerical Flutter Prediction in Blade Wheels

A. Wheel 1

The calculation of work done by pressure was conducted for the first four natural modes. Each mode was analyzed in a full range of possible numbers of nodal diameters. Oscillations are specified in the form of forward (along the wheel rotation) or backward traveling wave. Amplitude was normalized such that the maximum blade stress was 5×10^7 Pa. As explained previously, we investigated two configurations of this wheel. The first, "shrouded", is a production wheel; in particular, shroud contact pairs are in a perfect contact. The other, "cantilever" wheel, has blade shrouds slightly cut to be out of contact with shrouds of the neighboring blades. This wheel represents wear of material in shroud contact pairs after long operation time. The first four frequencies and mode shapes are shown in Fig. 10 for both wheel configurations; it is implied that the disk does not influence the blade eigenmodes, hence the mode shapes do not depend on the nodal diameter m. It is seen, first, that the natural frequencies of the cantilever wheel are lower than those of the

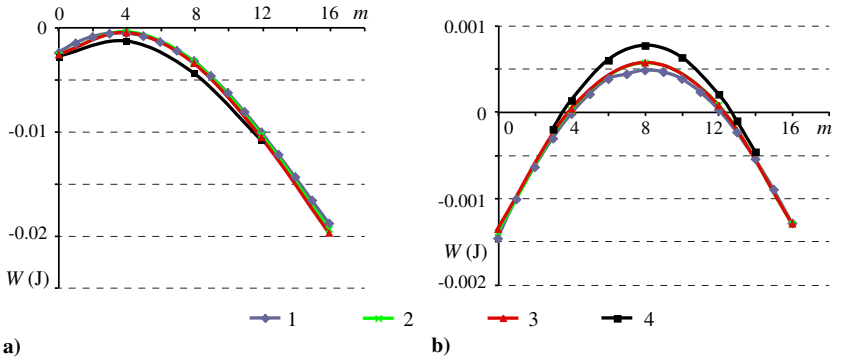

Fig. 9 Work vs m: a) mode 1, and b) mode 2. Curves 1–3: three-blade model, with different mesh sizes. Curve 4: five-blade model.

shrouded one due to the less overall stiffness of the structure. Second, and most important, in the range $n = 70 \ldots 80\%$, there is a mode shape exchange between the second and the third modes of cantilever blades; bending mode becomes torsional, and vice versa, which signifies a possible flutter occurrence. That is why flutter analysis has been conducted for $n = 80\%$, where the frequencies of the first four modes are 232, 576, 664, and 1328 Hz for cantilever blades and 683, 1069, 1501, and 2299 Hz for shrouded blades (note that the lowest mode in Fig. 10a cannot appear on a real wheel because the shroud has essentially nonzero displacement; this mode is excluded from consideration).

We assume that the cut of the blade shroud does not affect aerodynamics and use the same steady flow for both configurations. Work done over modes of cantilever blades is shown in Fig. 11. Work for the first and fourth modes is negative, whereas for the second and third modes it is positive for $m = 5 \ldots 11$ and $5 \ldots 16$, respectively. Therefore, for this wheel, we predict blade flutter in the second and third modes.

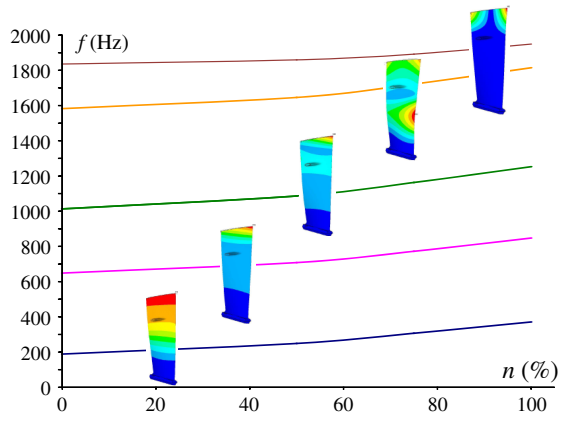

Fig. 10 Campbell diagram of wheel 1: a) shrouded, and b) cantilever. Blade contours represent relative displacement amplitude.

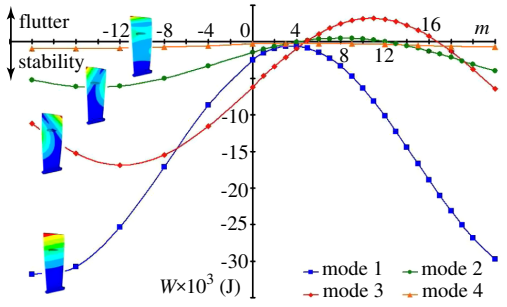

Fig. 11 Work done by unsteady pressure vs the number of nodal diameters for wheel 1 with cantilever blades.

Work calculated for the same wheel with shrouded blades is shown in Fig. 12. For the first four natural modes, the work is negative. We therefore predict the stability of this blade wheel.

The difference in flutter predictions for blades that are in and out of contact with each other through the midspan shroud leads us to a conclusion that a wheel that was initially designed to be flutter-free can actually flutter after some time of operation due to wear of material in the shroud and following change of the blade mode shapes and frequencies. To avoid this, the designer should determine safe operation period by taking into account change of modes and frequencies due to wear.

B. Wheel 2

Flutter analysis for the shrouded wheel 2 has been conducted for two operating regimes, corresponding to very close rotation speeds, $n = 94$ and 100%, which is why we used the same mode shapes and frequencies; the difference is only in aerodynamics. Blade eigenmode calculation was conducted with the disk elasticity taken into account; blades are in perfect contact through the shroud contact pairs. The resulting eigenmodes turned to be very sensitive to nodal diameters; the interference diagram is shown in Fig. 13. For the work calculation, we specified oscillation amplitude such that the maximum blade stress was 10^7 Pa. Work-per-cycle calculated for these modes is shown in Fig. 14c as "no tension" line. In contrast to wheel 1, it is not sinelike because each nodal diameter was modeled not only by a different phase shift but also by a different mode shape. It is seen that, for $m = 8 \ldots 10$, the work, though negative, comes close to zero, which means that the flutter boundary is somewhere close, and a slight change in the problem formulation can replace stability by flutter.

Such an important feature ignored so far is a shroud force. Indeed, when assembling the wheel, one should apply some force to a blade to make its shroud contacting with the neighboring blade shroud. As a result, in the assembled wheel, each blade is pretensioned by a force, which makes blades contacting each other through the shroud. Such a

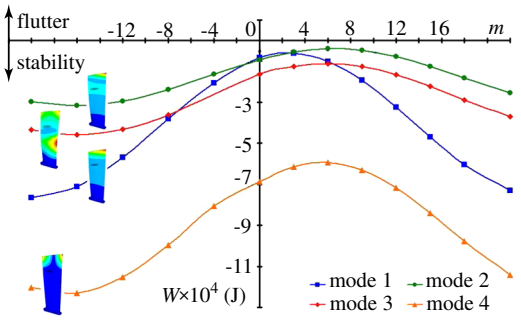

Fig. 12 Work done by unsteady pressure vs the number of nodal diameters for wheel 1 with shrouded blades.

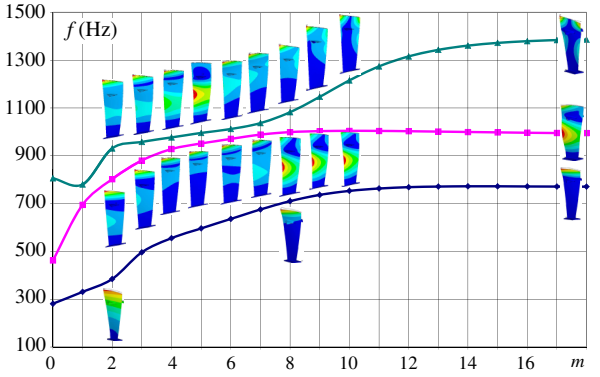

Fig. 13 Interference diagram of the wheel 2 at $n = 100\%$ (first three modes are shown).

Downloaded by UNIVERSITY OF CAMBRIDGE on August 21, 2015 | http://arc.aiaa.org | DOI: 10.2514/1.B35419

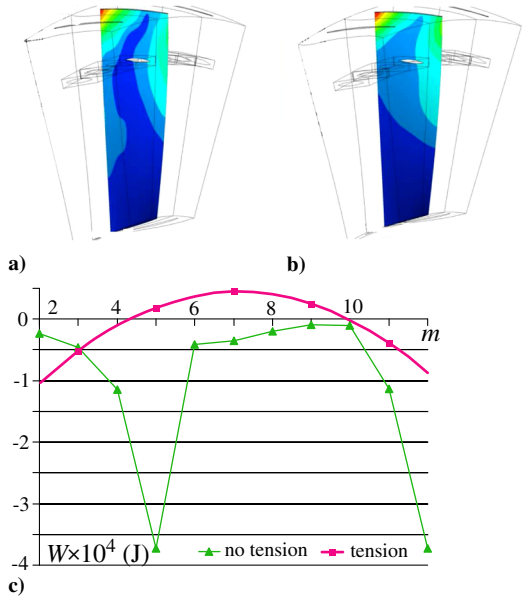

Fig. 14 Effect of shroud tension of the wheel 2 on the second mode at $n = 159.5$ Hz: a) tensioned blades ($m = 9$), b) untensioned blades, and c) work vs m.

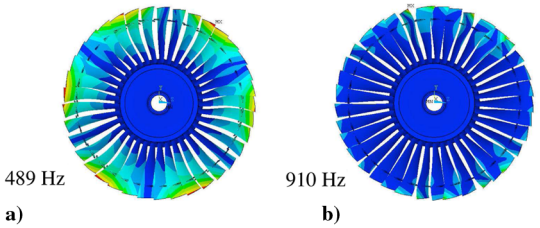

Fig. 15 Examples of natural modes calculated with shroud force taken into account: a) bending family, nodal diameters are clearly distinguished, and b) bending–torsional mode, no clear nodal diameters are seen.

tension can affect the mode shapes and change flutter prediction. Calculated mode shapes with shroud tension taken into account show that the first family of modes (bending modes, Fig. 15a) is close to those with no tension; however, the second and the third mode families (bending–torsional modes) are mixed, and one cannot clearly distinguish nodal diameters (Fig. 15b). In this situation, we took a blade mode that is closest to the one of untensioned wheel modes (namely, $m = 3$ for bending modes and $m = 9$ for bending–torsional modes) and changed nodal diameters without changing the mode shape and frequency. This simplified approach does not exactly represent the physics but gives a qualitative effect of the shroud tension. The tension turned out to be extremely important due to change of the mode shapes (Figs. 14a, 14b). Shown in Fig. 14c, by "tension" curve is the work calculated for a tensioned wheel in the manner described. It is seen that the prediction is changed from stability to flutter, which means that the shroud tension can significantly affect the result, at least near the flutter boundary.

Work done by unsteady pressure over the first two natural modes of tensioned wheel is shown in Fig. 16 by continuous curves. It is seen that both modes are damped at $n = 170$ Hz; hence, we predict stability, whereas at $n = 159.5$ Hz, the second mode ($f = 910$ Hz) with 5 . . . 9 nodal diameters is in flutter zone.

C. Influence of Midspan Shroud

Midspan shroud is a structure usually introduced to increase the damping of blades and change their natural modes, which is why it is necessary to take it into account when calculating static stress and natural modes and frequencies. On the other hand, it is a common practice to ignore midspan shroud when calculating steady airflow because the shape of the blade shroud is usually designed to affect the flow as little as possible. However, the influence of the shroud on unsteady airflow is not so clear, which is why we consider it in this section.

We investigated two models of the same wheel; the geometry of the first consists of the blade passage only, whereas the other includes geometry of the midspan shroud (note that the shroud is always modeled in modal analysis). Steady flow conditions, natural modes, and frequencies are the same and correspond to $n = 159.5$ Hz regime. Results are shown in Fig. 16 by continuous and dashed curves for the model with and without the shroud, respectively. It is seen that neglecting the midspan shroud in unsteady flow analysis increases the work for both modes for any number of nodal diameters. The same result was obtained for the work done for the untensioned wheel, which is not presented here. In other words, neglecting the shroud is conservative: if the shroud is ignored, then when one predicts stability, it is reinforced by the shroud; in the case of flutter, additional investigation with the shroud "aerodynamically" taken into account is necessary. We cannot, of course, make the same conclusion for any wheel, but results obtained for the wheel under consideration could be a good point to start checking shroud influence for other wheels.

D. Influence of Inlet Angle of Attack

One of the natural modes was used for the investigation of influence of the inlet angle of attack α. At each point of the inlet, the velocity direction was changed by a specified angle, whereas the absolute value of the velocity remained unchanged. The boundary values of other quantities, pressure and temperature, were not changed. Such an approach is only valid for a small change of α because any significant change of the angle of guide vanes changes the steady flow in all stages, whereas we assume that the change is localized in the wheel following the guide vanes. Thus, the result of such an investigation should not be used in design; however, for a small deviation of α, it gives a qualitative influence of the inlet angle of attack, which is useful to know.

The calculation was conducted for the second mode, $m = 9$, without taking midspan shroud tension into account. The model of

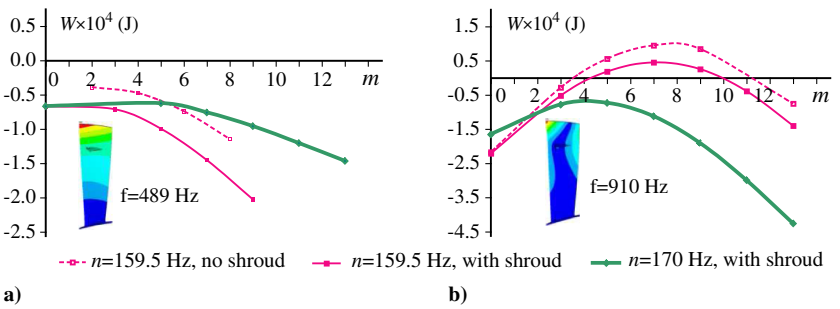

Fig. 16 Work done by unsteady pressure vs nodal diameter for wheel 2; effect of shroud modeling in aerodynamic analysis: a) first (bending) mode, and b) second (bending–torsional) mode.

Downloaded by UNIVERSITY OF CAMBRIDGE on August 21, 2015 | http://arc.aiaa.org | DOI: 10.2514/1.B35419

unsteady flow included the shroud. The results of the analysis are shown in Fig. 17. It is seen that a deviation of the angle by 4 deg or less insignificantly changes work-per-cycle, especially compared with other numbers of nodal diameters (Fig. 14). A deviation by higher angles yields a positive work, which rapidly increases with the increase of $|\Delta\alpha|$. A possible explanation is the appearance of local stall zones. However, as was argued previously, such high angles require a steady flow recalculation in all stages of the compressor, and results of the present analysis in this case are hardly meaningful. We therefore conclude that a deviation of the inlet angle of attack caused by a change of guide vanes angle (due to manufacturing tolerances, wrong operating program, or other reasons) by 4 deg or less does not essentially affect flutter.

E. Influence of Blade Mode Shape Change Due to Manufacturing Tolerances

Let us now investigate the influence of manufacturing tolerances associated with the blade production or blade shape change in design.

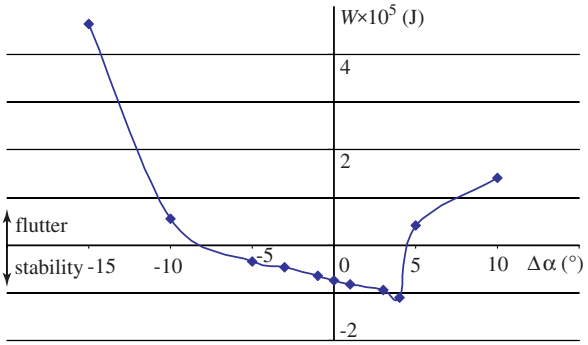

Fig. 17 Work-per-cycle vs deviation of the angle of attack from the design value for the second mode, $m = 9$ of wheel 2.

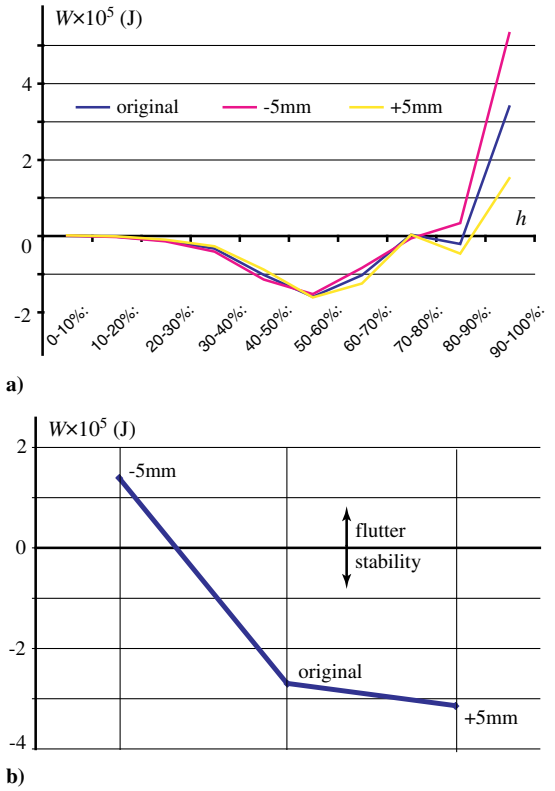

Fig. 18 a) Distribution of work-per-cycle along the blade span for original and shifted-to-the-root (−5 mm) and tip (+5 mm) mode shapes, and b) total work-per-cycle.

First, consider the distribution of work done by pressure along the blade span. This distribution is important when redesigning the blade to avoid flutter. Shown as "original" in Fig. 18a is the distribution of the work for the second mode $m = 10$. Blade mode shapes are calculated without modeling the shroud tension. An analysis of unsteady aerodynamics is conducted with taking the shroud into account. It is seen that the most positive values of the work are achieved at the blade tip. However, the total work for the blade is negative (Fig. 18b) because of the region of negative work at 40 . . . 80% of the span, where the blade dissipates the energy, which in total exceeds the amount of income energy at 90 . . . 100% of the span.

However, small changes of nodal line locations (for example, due to tolerance for the blade thickness or blade twisting angle) can change this balance and change the sign of the total work due to the change of the tip region length where the work is positive. To check this hypothesis, we calculated the work for the mode shape shifted by ±5 mm along the span, without changing the steady flow. Second mode of the wheel 2 blade with m = 10 is studied. The shift was introduced by changing the interpolated mode shape function; the z coordinate directed along the blade span was replaced by $z + 0.005$ to $z - 0.005$ m, respectively. The distribution of the work along the blade span is shown in Fig. 18a. It is seen that the tip region size, where the work is positive, and the amount of work are increased or decreased depending on the direction of the mode shape shift. The total work-per-cycle done for the whole blade is shown in Fig. 18b for original and shifted mode shapes. It is seen that, because of the change of the work done at the blade tip region, total work becomes positive for the mode shifted to the blade root. We conclude that even a relatively small shift of the nodal lines (by 5 mm) due to manufacturing tolerances or other reasons can yield flutter. If such a situation occurs for the original blade, one could recommend a redesign of the blade shape such that nodal lines are shifted to the blade tip. Thus, the mode shape can significantly change flutter prediction, and its change can be an efficient way to avoid flutter.

The distribution of work along the blade span shown in Fig. 18a gives also an important example when results of 2-D and 3-D flutter analyses are different. Indeed, in the practice of jet engine developers and in academic studies, the problem is often considered in 2-D formulation, for the blade cross section at 80 . . . 100% of the blade span. It is assumed that such 2-D analysis drives the total instability of the blade. However, Fig. 18 shows a blade, which is stable, but its cross section at 90 . . . 100% transfers energy from the flow to the blade. In other words, a 2-D analysis of this blade would predict flutter, whereas a 3-D analysis predicts stability. Obviously, one could find other blades with such mode shape that a 2-D analysis would predict stability, whereas 3-D would predict flutter.

V. Experimental Validation of Numerical Results

The validation of numerical flutter prediction for wheels 1 and 2 was conducted at special full-scale tests of the gas-turbine engine.

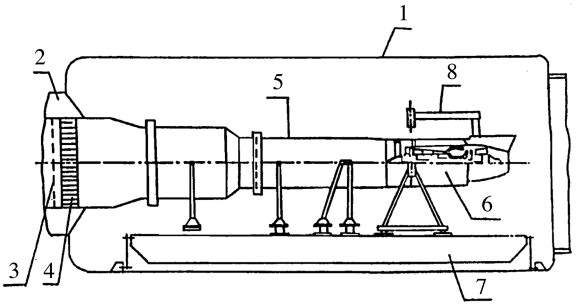

Fig. 19 Sketch of the test facility for blade flutter detection during engine test: 1) altitude chamber, 2) receiver, 3) honeycomb, 4) mesh, 5) piping, 6) engine, 7) force meter platform, and 8) engine mounting.

Downloaded by UNIVERSITY OF CAMBRIDGE on August 21, 2015 | http://arc.aiaa.org | DOI: 10.2514/1.B35419

Downloaded by UNIVERSITY OF CAMBRIDGE on August 21, 2015 | http://arc.aiaa.org | DOI: 10.2514/1.B35419

A. Test Facility, Strain Gauge Locations, and Test Procedure

An experimental detection of compressor blade flutter was conducted using a special test facility (Fig. 19) with a simulation of altitude, speed, and environmental air conditions, including required flow irregularity, flow pressure, and temperature at the engine inlet.

Airflow at the inlet of the fan has average values of the total pressure and stagnation temperature equal to the averaged values of the parameters of the fan operating at flight conditions on an aircraft with required margins of safety. From a compressor station, the air flows through refrigerating units or air heaters providing required pressure and temperature values.

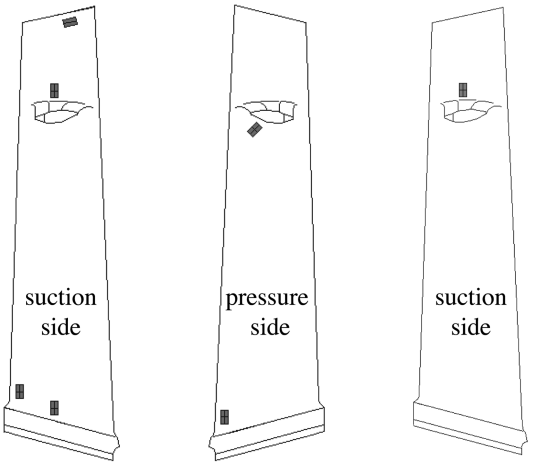

Fig. 20 Strain gauge locations on tested blades: a) wheel 1, and b) wheel 2.

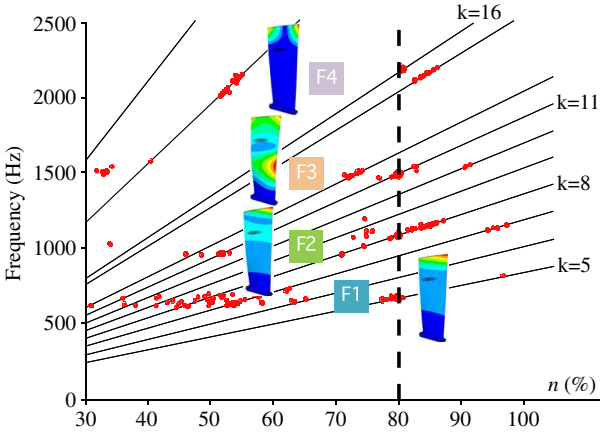

Fig. 21 Strains measured for shrouded blade wheel 1 (Campbell diagram). Dots represent spectral peaks with amplitudes exceeding noise level.

The blades of wheels 1 and 2 were prepared with strain gauges located in the regions of maximum stress for the first four natural modes, which are usually most unstable (Fig. 20). The maximum stress zones for these modes were obtained by a numerical study and during laboratory tests on a vibration-testing machine. To perform a phase shift analysis for the detection of a number of nodal diameters in coupled blade–disc–flow vibrations, several consecutive blades were prepared with strain gauges.

A multichannel high-efficiency recording apparatus was used to record and control data from the strain gauges. It provides the required discretization frequency of signal processing with a spectral resolution of 1 Hz and an amplitude accuracy of 2%. The connection between strain gauges and processing apparatus is established through a multichannel remote converter.

The processing of data from strain gauges consisted of the analysis of spectral structure and the correlation analysis of data from consecutive blades using narrowband spectral analysis.

B. Test Results

As well as in numerical analysis, two modifications of wheel 1 were tested: blades with midspan shroud and cantilever blades. Based on the analysis of strain gauge data from the shrouded wheel, no flutter was detected in the whole range of the fan speed. At two speed ranges, the vibration amplitudes were at increased but still acceptable levels. First, at $n = 40 \ldots 60\%$ (i.e., at relatively low rotation speeds, where the flow is unstable), random forced vibrations with low amplitudes were detected. Second, at $n = 80\%$, resonant vibrations occurred in the first four modes with an acceptable level of stress amplitudes (Fig. 21).

However, signal processing from the strain gauges of wheel 1 with cantilever blades shows that starting from rotor speed $n = 55\%$, nonresonant vibrations occur in modes 2, 3, and 4 with a high total level of vibration stress (Fig. 22a). Spectral and correlation analysis from both neighboring and remote blades shows flutter onset in second ($m = 6 \ldots 7$) and third ($m = 5 \ldots 14$) natural modes (Fig. 22b). Based on correlation analysis, oscillations in the fourth mode were classified as random forced vibrations.

Thus, test results of wheel 1 are in full agreement with the numerical predictions (Sec. IV.A). Indeed, the predicted stability and flutter regimes coincide with the test stability and flutter regimes; moreover, flutter was observed in the same modes and nodal diameters as predicted to be unstable (compare Figs. 11, 22b).

The test results for wheel 2 were obtained for the full range of rotation speeds; inlet airflow parameters included regimes with heating and compressing the flow. During the test, flutter was detected at the regime $n = 159.5$ Hz with a dominating frequency of 906 Hz (Fig. 23). Signal processing showed that vibrations occurred in the second mode with forward traveling wave and a number of nodal diameters $m = 6 \ldots 8$. Pressure gauges installed on the casing over the wheel detected forward traveling rotating pressure wave with $m = 8$. At other operating regimes, including $n = 170$ Hz, no flutter was detected. These results demonstrate excellent agreement

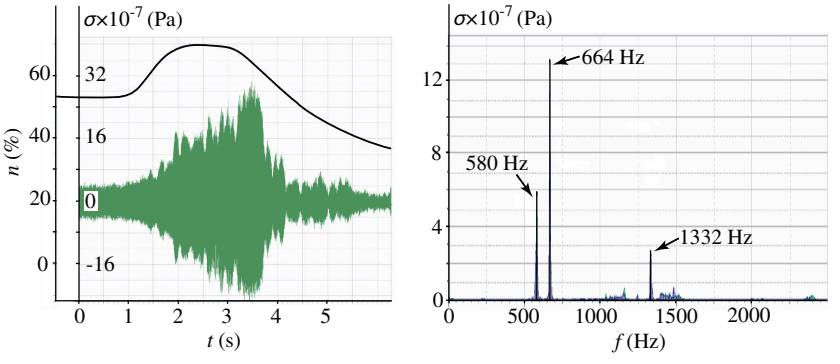

Fig. 22 Test results of the cantilever blade wheel 1: a) rotation speed and blade stress, and b) spectrum of the blade stress during flutter.

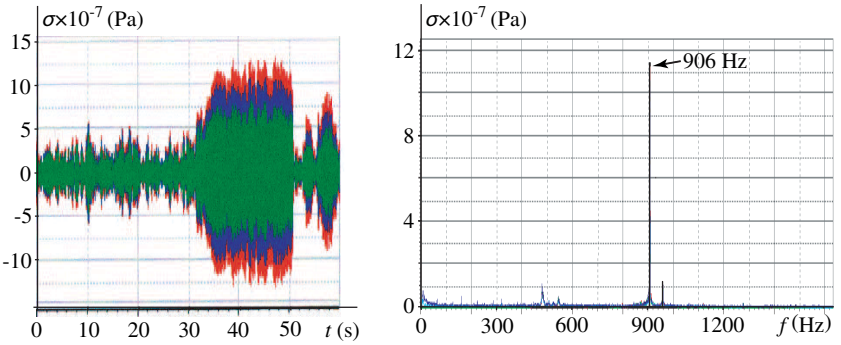

Fig. 23 Test results of the wheel 2 at $n = 159.5$ Hz: a) blade stress (data from different blades with the same strain gauge location), and b) spectrum of the blade stress during flutter.

between test data and the numerical prediction of flutter onset (Fig. 16b) for the wheel considered.

Good correlation between numerical and test data for both wheels considered validates the procedure and the workflow developed, which will be used in the design of new compressor blades.

VI. Conclusions

A flutter prediction procedure based on the energy method has been developed. It is valid for the unstalled flow conditions, which are typical for operating regimes. Two examples of application of this procedure to real blade wheels are given. Both are verified by full-scale tests in two operating regimes: stable and flutter.

The influence of numerical parameters, as well as blade design parameters and assembling conditions on flutter onset, is studied. It is shown that there is no significant influence of increased numerical accuracy and flow angle of attack variation within manufacturing tolerance. Tension in the midspan shroud has a considerable effect on the predicted flutter onset, although the inclusion of the midspan shroud in the unsteady aerodynamic model does not have significant effect. It is shown that, for a reliable flutter prediction, it is enough to use the three-blade one-stage aerodynamic model and to calculate work done by unsteady pressure for the middle blade during the third oscillation period.

The parameters of the modeling experimentally verified in this paper can be used in the design of new compressors that have a nontypical blade or disc shape for the prediction of flutter onset. They are also suitable for blade wheel design or redesign for flutter suppression near compressor operating regimes with unstalled airflow.

Acknowledgments

The work is supported by the Russian Foundation for Basic Research (14-01-31547 and 14-01-00049) and grants NSh-3530.2014.1 and MD-4544.2015.1.

References

[1] Bolcs, A., and Suter, P., *Transsonische Turbomaschinen*, G. Braun Verlag, Karlsruhe, 1986.

[2] Bendiksen, O., "Recent Developments in Flutter Suppression Techniques for Turbomachinery Rotors," *Journal of Propulsion and Power*, Vol. 4, No. 2, 1988, pp. 164–171. doi:10.2514/3.51283

[3] Marshall, J. G., and Imregun, M., "A Review of Aeroelasticity Methods with Emphasis on Turbomachinery Applications," *Journal of Fluids and Structures*, Vol. 10, No. 3, 1996, pp. 237–267. doi:10.1006/jfls.1996.0015

[4] Shrinivasan, A. V., "Flutter and Resonant Vibration Characteristics of Engine Blades," *Journal of Engineering for Gas Turbines and Power*, Vol. 119, No. 4, 1997, pp. 742–775. doi:10.1115/1.2817053

[5] Petrie-Repar, P., McGhee, A., Jacobs, P., and Gollan, R., "Analytical Maps of Aerodynamic Damping as a Function of Operating Condition for a Compressor Profile," *Proceedings of the ASME Turbo Expo 2006*, American Soc. of Mechanical Engineers, New York, May 2006.

[6] Khorikov, A. A., and Danilkin, S. Y., "Research of the Fan Blades Flutter on the Stalling Airflow Mode," *Herald of Samara State Aerospace University*, Vol. 2, No. 3, 2011, pp. 57–63 (in Russian).

[7] Gnesin, V., and Rzadkowski, R., "A Coupled Fluid–Structure Analysis for 3-D Inviscid Flutter of IV Standard Configuration," *Journal of Sound and Vibration*, Vol. 251, No. 2, 2002, pp. 315–327. doi:10.1006/jsvi.2001.3981

[8] Godunov, S. K., Kurzin, V. B., Bunkov, V. G., and Sadkane, M., "Application of a New Mathematical Tool (1D Spectral Portraits of Matrices) to the Problem of Aeroelasticity Vibrations of Turbine Blade Cascades," *TsAGI Science Journal*, Vol. 40, No. 6, 2009, pp. 645–656. doi:10.1615/TsAGISciJ.v40.i6.20

[9] Lokshtanov, E. A., Mikhailov, V. M., and Khorikov, A. A., "Probabilistic Flutter Prediction of Turbomachine Blades," *Aeroelasticity of Turbomachine Blades*, Naukova Dumka, Kiev, Ukraine, 1980, pp. 73–81 (in Russian).

[10] Khorikov, A. A., "Prediction and Diagnostics of Blade Flutter in Axial Compressors of Jet Engines," *Proceedings of the Central Institute of Aviation Motors*, No. 1311, Moscow, 2002 (in Russian).

[11] Bartels, R. E., and Sayma, A. I., "Computational Aeroelastic Modelling of Airframes and Turbomachinery: Progress and Challenges," *Philosophical Transactions of the Royal Society A: Mathematical, Physical and Engineering Sciences*, Vol. 365, 2007, pp. 2469–2499. doi:10.1098/rsta.2007.2018

[12] Snyder, L. E., and Commerford, G. L., "Supersonic Unstalled Flutter in Fan Rotors: Analytical and Experimental Results," *Journal of Engineering for Gas Turbines and Power*, Vol. 96, No. 4, 1974, pp. 379–386. doi:10.1115/1.3445861

[13] Verdon, J. M., "Linearized Unsteady Aerodynamics for Turbomachinery Aeroelastic Applications," *Journal de Physique III*, Vol. 2, 1992, pp. 481–506. doi:10.1051/jp3:1992143

[14] Sadeghi, M., and Liu, F., "Computation of Mistuning Effects on Cascade Flutter," *AIAA Journal*, Vol. 39, No. 1, 2001, pp. 22–28. doi:10.2514/2.1297

[15] Reddy, T. S. R., Srivastava, R., and Mehmed, O., "ASTROP2-LE: A Mistuned Aeroelastic Analysis System Based on a Two Dimensional Linearized Euler Solver," NASA TM-2002-211499, 2002.

[16] Ferria, H., Ferrand, P., Delmas, L., and Aubert, S., "Numerical Investigation of Supersonic Flutter in Space Turbine Based on Unsteady Computations Linearized in the Frequency Domain in Response to a Prescribed Blade Motion," *Proceedings of the International Forum of Aeroelasticity and Structural Dynamics (IFASD)*, Association Aéronautique et Astronautique de France, Paris, 2011.

[17] Ekici, K., Kielb, R. E., and Hall, K. C., "The Effect of Aerodynamic Asymmetries on Turbomachinery Flutter," *Journal of Fluids and Structures*, Vol. 36, 2013, pp. 1–17. doi:10.1016/j.jfluidstructs.2012.08.009

[18] Kahl, G., and Hennings, H., "Computational Investigation of an Oscillating Compressor Cascade Experiment," *Proceedings of the 9th International Symposium on Unsteady Aerodynamics, Aeroacoustics and Aeroelasticity of Turbomachines (ISUAAAT)*, Presses Universitaires de Grenoble, Grenoble, 2000, pp. 819–829.

[19] Lepicovsky, J., McFarland, E. R., Capece, V. R., Jett, T. A., and Senyitko, R. G., "*Methodology of Blade Unsteady Pressure*

Downloaded by UNIVERSITY OF CAMBRIDGE on August 21, 2015 | http://arc.aiaa.org | DOI: 10.2514/1.B35419

Measurement in the NASA Transonic Flutter Cascade," NASA TM-2002-211894, 2002.

[20] Allegret-Bourdon, D., and Fransson, T. H., "Study of Shock Movement and Unsteady Pressure on 2D Generic Model," *Unsteady Aerodynamics, Aeroacoustics and Aeroelasticity of Turbomachines*, Springer, Dordrecht, 2006, pp. 409–421.

[21] Tsimbalyuk, V. A., "Method of Measuring Transient Aerodynamic Forces and Moments on Vibrating Cascade," *Strength of Materials*, Vol. 28, No. 2, 1996, pp. 150–157. doi:10.1007/BF02215842

[22] Stelmakh, A. L., Len, A. D., and Zinkovskii, A. P., "Experimental–Numerical Investigation of the Dynamic Stability of Flexural–Torsional Vibrations of Compressor Blades Under Conditions of Attached and Separated Flow, Part 1, Procedure and Equipment for the Determination of Nonstationary Aerodynamic Characteristics," *Strength of Materials*, Vol. 39, No. 2, 2007, pp. 200–210.

[23] Stelmakh, A. L., Len, A. D., and Zinkovskii, A. P., "Experimental–Numerical Investigation of the Dynamic Stability of Flexural–Torsional Vibrations of Compressor Blades Under Conditions of Attached and Separated Flow, Part 2, Cross Aerodynamic Characteristics," *Strength of Materials*, Vol. 41, No. 4, 2009, pp. 407–416.

[24] Stelmakh, A. L., Len, A. D., and Zinkovskii, A. P., "Experimental–Numerical Investigation of the Dynamic Stability of Flexural–Torsional Vibrations of Compressor Blades Under Conditions of Attached and Separated Flow, Part 3, Mutual Aerodynamic Couplings," *Strength of Materials*, Vol. 42, No. 3, 2010, pp. 304–312.

[25] Moyroud, F., Jacquet-Richardet, G., and Fransson, T. H., "Aeroelasticity in Turbomachines: Some Aspects of the Effect of Coupling Modeling and Blade Material Changes," *International Journal of Rotating Machinery*, Vol. 6, No. 4, 2000, pp. 265–273. doi:10.1155/S1023621X00000257

[26] Sayma, A. I., Vahdati, M., Green, J. S., and Imregun, M., "Whole-Assembly Flutter Analysis of a Low Pressure Turbine Blade," *Unsteady Aerodynamics and Aeroelasticity of Turbomachines*, Kluwer Academic Publ., Dordrecht, 1998, pp. 347–359.

[27] Breard, C., Imregun, M., Sayma, A., and Vahdati, M., "Flutter Stability Analysis of a Complete Fan Assembly," *37th Aerospace Sciences Meeting and Exhibit*, AIAA Paper 1999-0238, Jan. 1999.

[28] Vahdati, M., Sayma, A. I., Marshall, J. G., and Imregun, M., "Mechanisms and Prediction Methods for Fan Blade Stall Flutter," *Journal of Propulsion and Power*, Vol. 17, No. 5, 2001, pp. 1100–1108.

[29] Vahdati, M., Sayma, A. I., Breard, C., and Imregun, M., "Computational Study of Intake Duct Effects on Fan Flutter Stability," *AIAA Journal*, Vol. 40, No. 3, 2002, pp. 408–418. doi:10.2514/2.1680

[30] Srivastava, R., Bakhle, M. A., Keith, T. G., Jr., and Stefko, G. L., "*Flutter Analysis of a Transonic Fan*," NASA TM-2002-211818, 2002.

[31] Reddy, T. S. R., Bakhle, M. A., Trudell, J. J., Mehmed, O., and Stefko, G. L., "*LINFLUX-AE: A Turbomachinery Aeroelastic Code Based on a 3-D Linearized Euler Solver*," NASA TM-2004-212978, 2004.

[32] Kurzin, V. B., and Tolstukha, A. S., "Calculation of the Unsteady Aerodynamic Parameters of a Rotating Cascade of Oscillating Blades in Incompressible Flow," *Fluid Dynamics*, Vol. 40, No. 1, 2005, pp. 34–45. doi:10.1007/s10697-005-0041-4

[33] Campobasso, M. S., and Giles, M. B., "Stabilizing Linear Harmonic Flow Solvers for Turbomachinery Aeroelasticity with Complex Iterative Algorithms," *AIAA Journal*, Vol. 44, No. 5, 2006, pp. 1048–1059. doi:10.2514/1.17069

[34] May, M., Maurey, Y., and Sicot, F., "Numerical Flutter Analysis of Turbomachinery Bladings on Time-Linearized, Time-Spectral and Time-Accurate Simulations," *Proceedings of the International Forum of Aeroelasticity and Structural Dynamics (IFASD)*, Association Aéronautique et Astronautique de France, Paris, 2011.

[35] He, Z., Epureanu, B. I., and Pierre, C., "Fluid–Structural Coupling Effects on the Dynamics of Mistuned Bladed Disks," *AIAA Journal*, Vol. 45, No. 3, 2007, pp. 552–561. doi:10.2514/1.23809

[36] Placzek, A., and Dugeai, A., "Numerical Prediction of the Aeroelastic Damping Using Multi-Modal Dynamically Coupled Simulations of a 360 Fan Configuration," *Proceedings of the International Forum of Aeroelasticity and Structural Dynamics (IFASD)*, Association Aéronautique et Astronautique de France, Paris, 2011.

[37] Martensson, H. E., Ostlund, J., Bladh, R., and Gruber, B., "Design and Analysis of a Transonic Flutter Research Compressor," *Proceedings of the International Forum of Aeroelasticity and Structural Dynamics (IFASD)*, Association Aéronautique et Astronautique de France, Paris, 2011.

[38] Vogt, D. M., and Fransson, T. H., "Towards Flutter-Free Turbomachinery Blades," " Innovations for Sustainable Aviation in a Global Environment," IOS Press, Amsterdam, 2012, pp. 161–167.

[39] Nowinski, M., and Panovsky, J., "*Flutter Mechanisms in Low-Pressure Turbine Blades*," American Soc. of Mechanical Engineers Paper 98-GT-573, New York, 1998.

[40] Silkowski, P. D., Rhie, C. M., Copeland, G. S., Eley, J. A., and Bleeg, J. M., "*CFD Investigation of Aeromechanics*, " American Soc. of Mechanical Engineers Paper 2001-GT-0267, New York, 2001.

[41] McBean, I., Hourigan, K., Thompson, M., and Liu, F., "Prediction of Flutter of Turbine Blades in a Transonic Annular Cascade," *Journal of Fluids Engineering*, Vol. 127, No. 6, 2005, pp. 1053–1058. doi:10.1115/1.2060731

[42] Bakhle, M. A., Reddy, T. S. R., and Stefko, G. L., "Comparisons of Flutter Analyses for an Experimental Fan," NASA TM-2010-216221, 2010.

[43] Kolotnikov, M. E., Makarov, P. V., and Sachin, V. M., "Study of Wide-Chord Blade Dynamic Strength During Tests," *Aviation and Space Techniques and Technology*, Vol. 56, No. 9, 2008, pp. 58–64 (in Russian).

[44] Kielb, R., Barter, J., Chernysheva, O., and Fransson, T., "Flutter Design of Low Pressure Turbine Blades with Cyclic Symmetry Modes," *Unsteady Aerodynamics, Aeroacoustics and Aeroelasticity of Turbomachines*, Springer, Dordrecht, 2006, pp. 41–52.

[45] Samoylovich, G. S., *Unsteady Flow and Aeroelastic Vibrations in Turbomachine Cascades*, Nauka, Moscow, 1969, pp. 181–198 (in Russian).

J. Bons
Associate Editor

Downloaded by UNIVERSITY OF CAMBRIDGE on August 21, 2015 | http://arc.aiaa.org | DOI: 10.2514/1.B35419